JACS
JOURNAL OF THE AMERICAN CHEMICAL SOCIETY

pubs.acs.org/JACS

Communication

Reversible Capture and Release of a Ligand Mediated by a Long-Range Relayed Polarity Switch in a Urea Oligomer

Steven M. Wales, David T. J. Morris, and Jonathan Clayden*

Cite This: *J. Am. Chem. Soc.* 2022, 144, 2841−2846

Read Online

ACCESS | Metrics & More | Article Recommendations | Supporting Information

ABSTRACT: Ethylene-bridged oligoureas characterized by a continuous, switchable chain of hydrogen bonds and carrying a binding site (an N,N′-disubstituted urea) for a hydrogen-bond-accepting ligand (a phosphine oxide) were synthesized. These oligomers show stronger ligand binding when the binding site is located at the hydrogen-bond-donating terminus than when the same binding site is at the hydrogen-bond-accepting terminus. An acidic group at the terminus remote from the binding site allows hydrogen bond polarity, and hence ligand binding ability, to be controlled remotely by a deprotonation/reprotonation cycle. Addition of base induces a remote conformational change that is relayed through up to five urea linkages, reducing the ability of the binding site to retain an intermolecular association to its ligand, which is consequently released into solution. Reprotonation returns the polarity of the oligomer to its original directionality, restoring the function of the remote binding site, which consequently recaptures the ligand. This is the first example of a synthetic molecular structure that relays intermolecular binding information, and these "dynamic foldamer" structures are prototypes of components for chemical systems capable of controlling chemical function from a distance.

The ability to relay, amplify, and process information distinguishes molecular systems in a biological context from those that are purely chemical.[1−4] Information processing in biology involves intermolecular interactions, either between biological macromolecules[5] or between a macromolecule and a small ligand,[6,7] with messages transmitted by way of conformational changes that propagate through those macromolecules.[8,9]

Communication devices[10] of this type are commonplace in biology,[11−14] and analogous spatial molecular communication has been achieved in synthetic molecules by induction of conformational changes at the terminus of an oligomeric structure.[15−17] Examples have involved communication of chirality through contiguous atropisomeric axes[18] or the screw-sense preference of a helix[19] or communication of polarity through a flexible chain of hydrogen bonds.[20,21] Without exception, such synthetic communication devices either exploit *intra*molecular interactions[22,23] or undergo irreversible change through chemical reaction,[12,13,24] precluding more general and reversible chemical function. To date, there is no artificial molecular communication device that allows continuous remote control of *inter*molecular interactions commonly seen in biology.

Here we report a molecular communication device that enables the control of noncovalent and reversible intermolecular interactions by a signal that is transmitted through a conformational change. Our general design concept is illustrated in Figure 1. An oligomeric structure in its "native state" (a) carries a terminal binding site that selectively binds a ligand. On input of a signal remote from the binding site (b), a conformational change is communicated to the binding site, disrupting binding and releasing the ligand into solution (c). Ligand release is reversible: removal of the input signal allows the binding site to reassemble and the ligand to return to its bound state.

In this instance, the input signal is provided by a change in pH, which leads to the reversible deprotonation and reprotonation of a thiourea functional group that "translates" pH into conformational change by mutating from a hydrogen bond acceptor to a hydrogen bond donor. This switch in polarity reverses the directionality of a chain of hydrogen bonds linking a series of urea functions, which disrupts the intermolecular interaction of a hydrogen bond acceptor (a phosphine oxide) with a terminal binding site.

We chose as this terminal binding site an electron-deficient N,N′-disubstituted urea function (Ar = 3,5-bis(trifluoromethyl)phenyl, abbreviated as "BTMP urea").[25] To establish the ability of induced hydrogen bond polarity to govern the local conformation of the BTMP urea—and hence its availability for ligand binding—oligomers **1** and **2** were synthesized (Figure 2a) in which each polarity-controlling group (the thiourea hydrogen bond donor in **1** and the *N*,*N*′-dimethylurea hydrogen bond acceptor in **2**) is separated from the BTMP urea by a hydrogen-bonded chain of three trisubstituted ureas.[20] We expected these molecules to maximize the stability of their hydrogen-bonded network by adopting hydrogen-bonding patterns of opposite directionality.

Received: November 11, 2021
Published: February 10, 2022

https://doi.org/10.1021/jacs.1c11928
J. Am. Chem. Soc. 2022, 144, 2841−2846

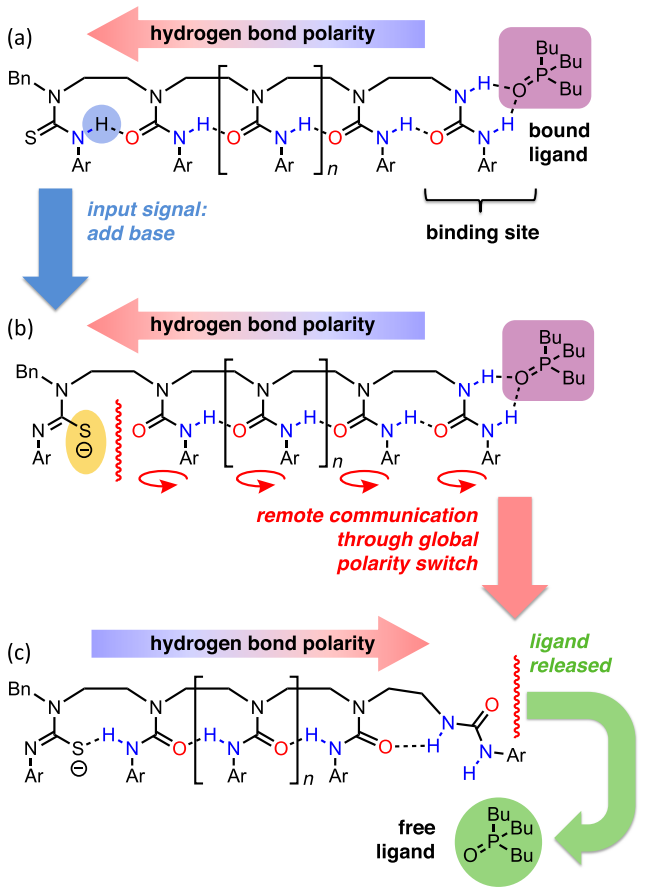

Figure 1. A conceptual framework for modulating ligand binding affinity through remote induction of global conformational changes.

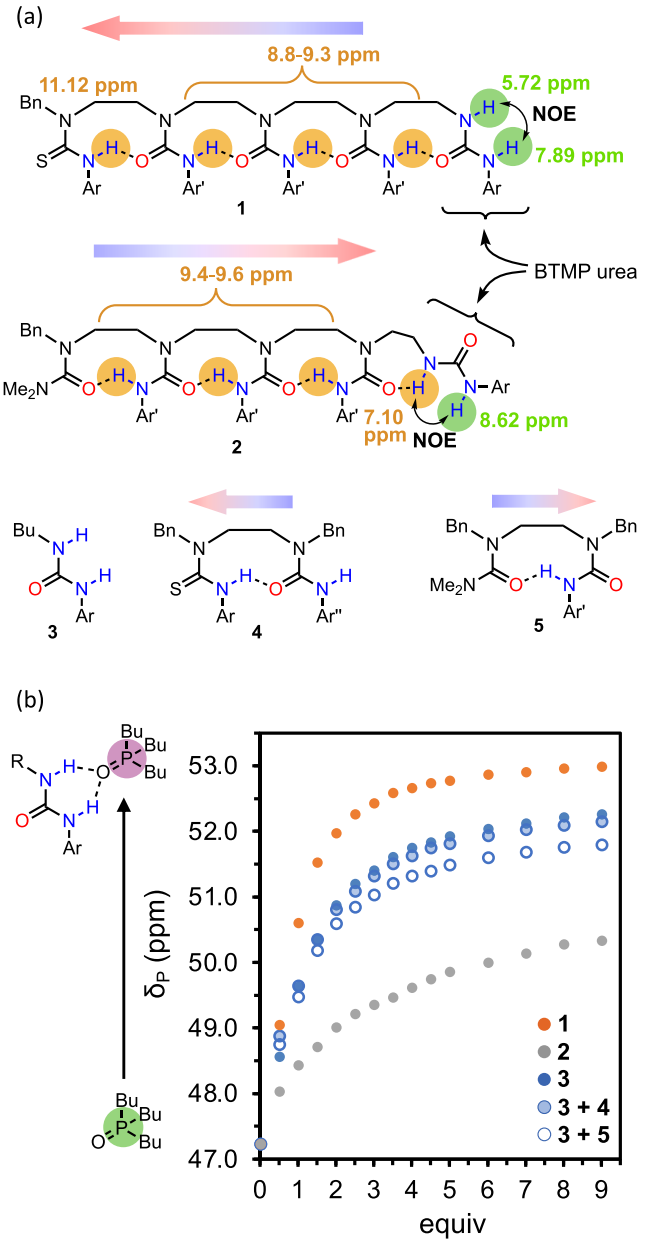

Figure 2. (a) BTMP ureas **1**–**5** (Ar = [3,5-$(CF_3)_2$]C_6H_3; Ar′ = *p*-$BuOC_6H_4$; Ar″ = *p*-$MeOC_6H_4$). (b) Titration experiments showing the change in the chemical shift in the ^{31}P NMR spectrum of Bu_3PO (2 mM, CH_2Cl_2) when titrated with ureas (0–9 equiv).

Oligomers **1** and **2** each showed a major conformer populated to ≥75% in CD_2Cl_2 (25 mM) at −10 °C (Figures S1–S11). In **1**, the more upfield chemical shifts of the alkyl and aryl N–H signals of the BTMP urea (Figure 2a: δ_H = 5.72 and 7.89 ppm, respectively) indicate that these (green) N–Hs are not involved in intramolecular hydrogen bonding, while in **2**, the (orange) alkyl N–H signal appears significantly further downfield (δ_H = 7.10 ppm) due to hydrogen bonding to the adjacent urea carbonyl group. In both **1** and **2**, a strong NOE correlation between the N–H signals of the BTMP urea (Figures S5 and S11) shows that the binding site adopts a *syn,syn* conformation, with the N–H bonds orientated parallel to one another. In **1**, these N–H bonds are available for intermolecular hydrogen bonding, while **2** cannot bind an external ligand without breaking an intramolecular hydrogen bond. The conformational distribution of **1** is largely insensitive to concentration and the number and identity of the internal urea linkages but does vary notably with solvent (Table S1).

Differences in the binding properties of **1** and **2** were explored by ^{31}P NMR using the strong hydrogen bond acceptor Bu_3PO (β = 10.7).[26,27] Titration of Bu_3PO with **1** and **2** (0–9 equiv) in CH_2Cl_2 (2 mM) resulted in values of $\Delta\delta_P$ (from the initial δ_P = 47.23 ppm) of +5.76 and +3.11 ppm, respectively (Figure 2b). A 1:1 binding model gave binding constants of 1490 ± 82 M^{-1} (for **1**) and 311 ± 21 M^{-1} (for **2**),[28] showing that **1** binds the phosphine oxide almost 5 times more strongly than **2**. The BTMP urea is itself a powerful hydrogen bond donor,[20] but these results demonstrate that the even more strongly hydrogen-bond-donating thiourea in **1** can override the BTMP urea's hydrogen-bonding preference.

Further information about binding was gained by using model compounds **3**–**5**. N,N′-Disubstituted urea **3**, an isolated binding site, has a Bu_3PO binding constant of 715 ± 16 M^{-1} ($\Delta\delta_P$ at 9 equiv = +5.04 ppm), showing that binding is enhanced by the "matched" polarity of **1** and weakened by the "mismatched" polarity of **2**. Under the same conditions, titrations of Bu_3PO with a 1:1 mixture of **3** and **4** (an isolated thiourea function), as well as a 1:1 mixture of **3** and **5** (an isolated *N,N′*-dimethylurea function), gave similar binding curves to **3** alone.[29] Neither **4** nor **5** alone (5 equiv) had any significant effect on the ^{31}P NMR chemical shift of Bu_3PO ($\Delta\delta_P$ < 0.4 ppm, Figures S35 and S37), confirming that the values of $\Delta\delta_P$ observed in all titrations (Figure 2b) are solely

https://doi.org/10.1021/jacs.1c11928
J. Am. Chem. Soc. 2022, 144, 2841–2846

due to binding of Bu_3PO to the BTMP urea. Collectively, these results confirm that the opposing polarities of the hydrogen bond chains in **1** and **2**, and the conformational preferences consequently induced in the BTMP urea, are responsible for their differing binding affinities to Bu_3PO.

Using this information, we designed a communication device in which a BTMP urea is switched remotely between the role of a hydrogen-bond donor and a hydrogen-bond acceptor in response to an external input. Switchable control was enabled by a relatively acidic thiourea that in its neutral form acts as a powerful hydrogen bond donor but on treatment with base is deprotonated to reveal a hydrogen-bond-accepting thiourea anion. Representative thiourea **4** provided a model of this behavior. ^{1}H NMR spectroscopy in CD_2Cl_2 confirmed that the thiourea N−H (δ_H = 10.58 ppm) hydrogen bonds strongly with the adjacent urea carbonyl (Figure 3). Consequently, the

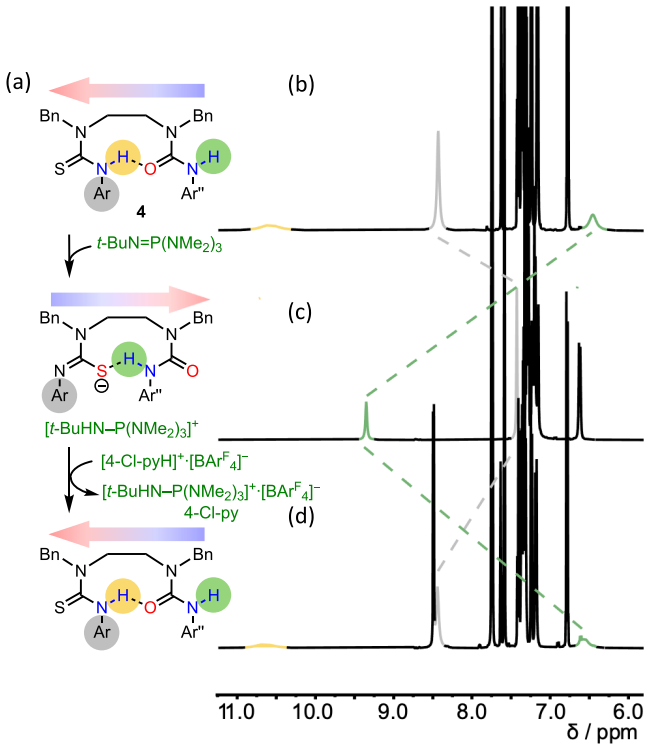

Figure 3. (a) Base-mediated hydrogen bond polarity switching of thiourea transmitter **4**. (b) ^{1}H NMR spectrum of **4** in CD_2Cl_2 at 42 mM, (c) with the addition of *t*-BuN=P(NMe$_2$)$_3$ (1 equiv) and (d) on addition of [4-Cl-pyH]$^+$·[BAr$^F_4$]$^-$ (1 equiv). Ar = Ar^F = [3,5-(CF$_3$)$_2$]C$_6$H$_3$; Ar″ = *p*-MeOC$_6$H$_4$.

N−H of the adjacent urea (δ_H = 6.46 ppm) forms no intramolecular hydrogen bond. Upon deprotonation of the thiourea with 1 equiv of phosphazene base *t*-BuN=P(NMe$_2$)$_3$ (chosen because the conjugate acid [*t*-BuHN−P(NMe$_2$)$_3$]$^+$ is a poor hydrogen bond donor), loss of the thiourea N−H signal (yellow) is accompanied by upfield shifts of the thiourea aryl protons (gray) and an upfield shift of the thiocarbonyl signal in the ^{13}C NMR spectrum (Figure S26). Concurrently, the urea N−H signal (green) shifts downfield to δ_H = 9.35 ppm ($\Delta\delta_H$ = +2.89 ppm), marking the formation of a strong hydrogen bond to the resultant thiourea anion and a switch in hydrogen-bond polarity. Reprotonation of the thiourea anion in the same mixture with 1 equiv of [4-Cl-pyH]$^+$·[BAr$^F_4$]$^-$ returned the NMR signals of **4** to their original positions, demonstrating that the byproducts [*t*-BuHN−P(NMe$_2$)$_3$]$^+$·[BAr$^F_4$]$^-$ and 4-chloropyridine do not interfere with the native hydrogen bonding in **4**.

The relayed effect of deprotonating the thiourea function of **1** on the terminal binding of the BTMP urea to Bu_3PO was investigated by using ^{31}P NMR spectroscopy (Figure 4). First,

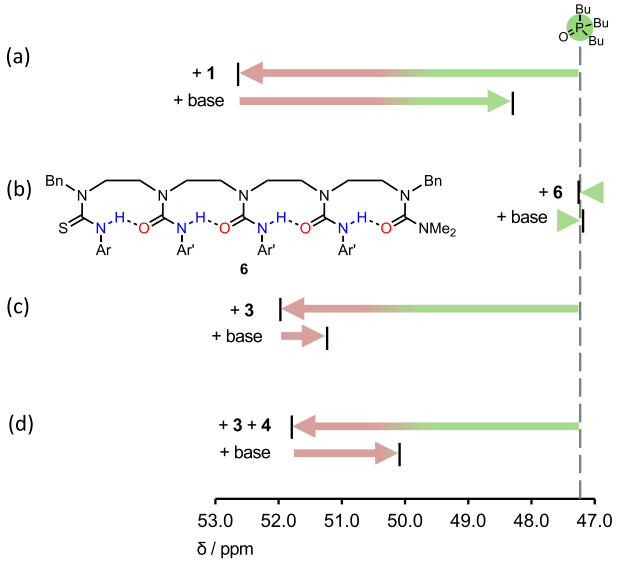

Figure 4. ^{31}P NMR chemical shift of Bu_3PO (2 mM, CD_2Cl_2) when treated with 5 equiv of a variant urea oligomer (namely (a) **1**, (b) **6**, (c) **3**, and (d) **3** and **4**) followed by 5 equiv of *t*-BuN=P(NMe$_2$)$_3$. Ar = [3,5-(CF$_3$)$_2$]C$_6$H$_3$; Ar′ = *p*-BuOC$_6$H$_4$.

1 (5 equiv) was added to bind the Bu_3PO, resulting in a downfield shift from δ_P = 47.23 ppm (free Bu_3PO) to δ_P = 52.66 ppm ($\Delta\delta_P$ = +5.43 ppm: Bu_3PO 92% bound, Figure S17). Upon addition of equimolar *t*-BuN=P(NMe$_2$)$_3$, deprotonation of the thiourea of **1** (Figure S31) was accompanied by a new signal arising from [*t*-BuHN−P(NMe$_2$)$_3$]$^+$·**1**$^-$ in the ^{31}P NMR spectrum (Figure S30).[30] Simultaneously, the Bu_3PO signal shifted upfield to δ_P = 48.31 ppm ($\Delta\delta_P$ = −4.35 ppm) (Figure 4a), consistent with the release of Bu_3PO from the remote binding site as a result of thiourea deprotonation (Figure S31).

Additional control experiments (Figure 4b−d) confirmed that induced release of Bu_3PO results from a relayed polarity switch. Bu_3PO was treated with a series of modified urea oligomers (5 equiv), each lacking one or more components of the integrated communication system, followed by *t*-BuN=P(NMe$_2$)$_3$ (5 equiv). Oligomer **6**, whose binding site is blocked by alkylation, was unable to bind Bu_3PO, and minimal $\Delta\delta_P$ resulted with either **6** or **6** + *t*-BuN=P(NMe$_2$)$_3$ (Figure 4b, Figures S38 and S39). This result confirms that the conjugate acid [BuHN−P(NMe$_2$)$_3$]$^+$ is itself unable to hydrogen bond to Bu_3PO. The isolated urea **3** binds Bu_3PO ($\Delta\delta_P$ = +4.76 ppm, Figure S32) but is resistant to deprotonation by *t*-BuN=P(NMe$_2$)$_3$ (Figure 4c and Figure S32). When Bu_3PO was complexed to **3** in the presence of **4** ($\Delta\delta_P$ = +4.58 ppm)—representing a "broken" device with a disconnected binding site—addition of base (Figure 4d, Figures S33 and S34) was accompanied by a modest upfield shift of Bu_3PO ($\Delta\delta_P$ = −1.71 ppm), indicating weakly competitive intermolecular binding of **3** to the thiourea anion of **4**$^-$, which partially liberates the phosphine oxide.[31]

https://doi.org/10.1021/jacs.1c11928
J. Am. Chem. Soc. 2022, 144, 2841−2846

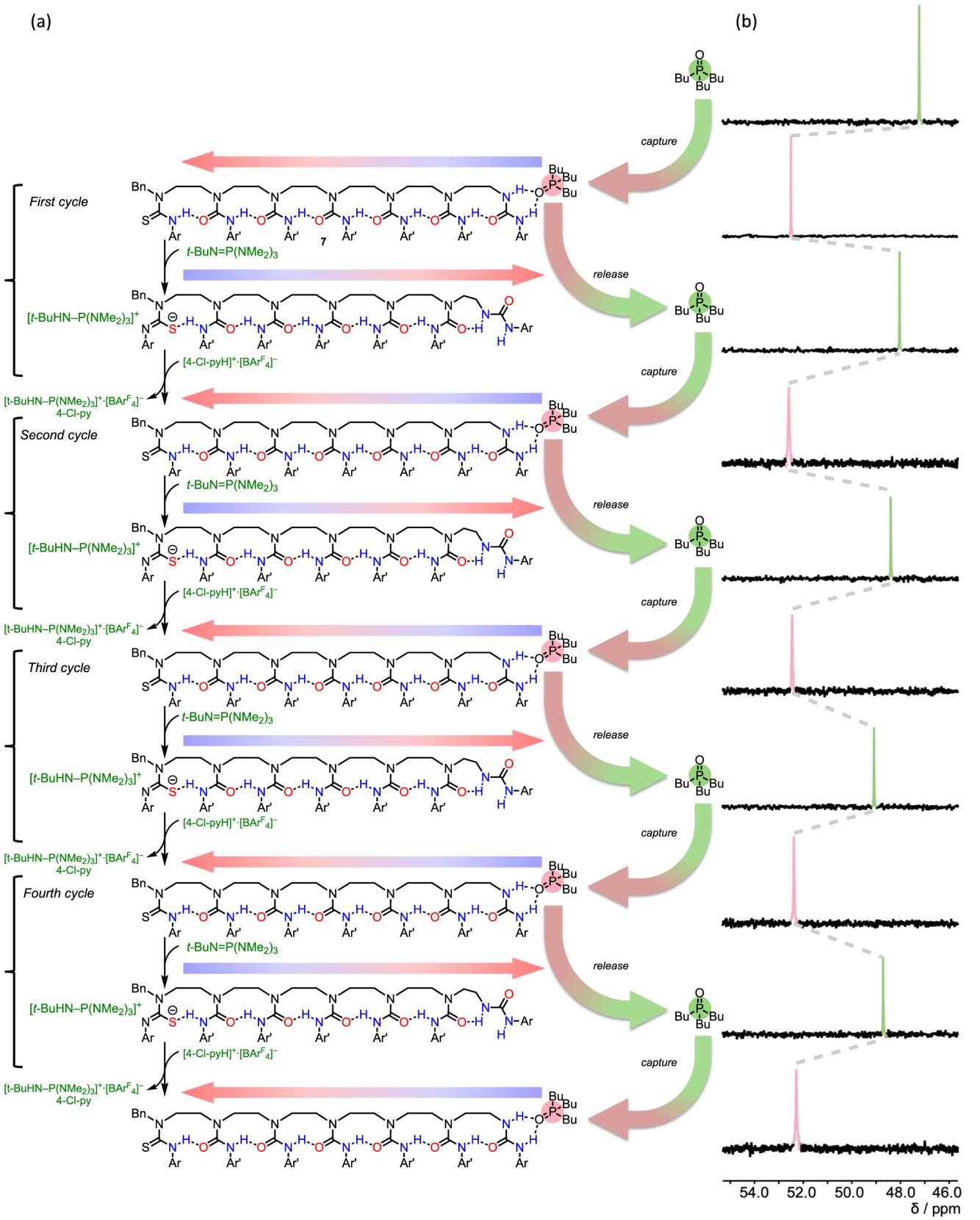

Figure 5. (a) Base-sensitive thiourea-capped oligomer **7** functioning as a ligand-capturing device. **7** captures Bu_3PO by hydrogen bonding at its terminal disubstituted urea binding site. Deprotonation of the remote thiourea with *t*-BuN═$P(NMe_2)_3$ transmits a global polarity change to the disubstituted urea which releases the phosphine oxide; reprotonation with $[4\text{-Cl-pyH}]^+\cdot[BAr^F{}_4]^-$ recaptures the phosphine oxide. (b) Characteristic changes in the ^{31}P NMR chemical shift of Bu_3PO (2 mM, CD_2Cl_2) on adding **7** (5 equiv), followed by repeated sequential additions of *t*-BuN═$P(NMe_2)_3$ (5 equiv) and $[4\text{-Cl-pyH}]^+\cdot[BAr^F{}_4]^-$ (5 equiv). Ar = Ar^F = $[3,5\text{-}(CF_3)_2]C_6H_3$; Ar′ = *p*-$BuOC_6H_4$.

https://doi.org/10.1021/jacs.1c11928
J. Am. Chem. Soc. 2022, 144, 2841−2846

A fully functioning device capable of reversible induced capture and release of a ligand over multiple cycles was demonstrated with the homologous oligourea **7**, which communicates information through a hydrogen-bonded chain of five internal ureas (Figure 5). The protonation state of the transmitting thiourea, which remotely controls the receiver's binding affinity for the ligand, was monitored by ^{1}H NMR (Figure S41), while the state of the ligand—bound or free—was simultaneously monitored by ^{31}P NMR.

The switching cycle started with the addition of **7** (5 equiv) to bind Bu_3PO (Figure 5), which induced a downfield shift (δ_P = 52.51 ppm, $\Delta\delta_P$ = +5.28 ppm) in the ^{31}P NMR spectrum. Thiourea deprotonation with *t*-BuN=P(NMe$_2$)$_3$ released this Bu_3PO back into solution ($\Delta\delta_P$ = −4.47 ppm). The ligand was then repeatedly recaptured and released by three sequential cycles of reprotonation with [4-Cl-pyH]$^+$·[BAr$^F_4$]$^-$ and deprotonation with *t*-BuN=P(NMe$_2$)$_3$ in one pot. Finally, the addition of further [4-Cl-pyH]$^+$·[BAr$^F_4$]$^-$ recaptured the Bu_3PO (δ_P = 52.28 ppm). Even after 4.5 capture and release cycles, communication device **7** maintains its binding function with minimal loss in efficiency.

In summary, a molecular communication device that can reversibly and remotely trigger a chemical response—namely the release and recapture of a ligand—has been realized. Information about the pH of an acidic thiourea's surroundings is converted to communicable hydrogen-bond polarity, which is relayed through a chain of hydrogen bonds to control the binding properties of a remote N,N′-disubstituted urea. Capture and release of the ligand can then be switched upon sequential treatment with acid and base several times in one pot. The remote modulation of an intermolecular interaction is reminiscent of actin treadmilling, suggesting future use of polarity reversal in the design of actin mimetics.[32] The ability to bind strong hydrogen bond acceptors, including Bu_3PO,[25] correlates strongly with catalytic activity in hydrogen bond donors,[33,34] suggesting that structures related to **1** and **7** might furthermore function as remotely switchable catalysts.

■ ASSOCIATED CONTENT

Supporting Information

The Supporting Information is available free of charge at https://pubs.acs.org/doi/10.1021/jacs.1c11928.

Synthetic schemes, experimental procedures and compound characterization data, details of conformational analysis, titration data and binding constant determination, ^{31}P and ^{1}H NMR spectra for capture and release experiments, and NMR spectra of novel compounds (PDF)

■ AUTHOR INFORMATION

Corresponding Author

Jonathan Clayden − *School of Chemistry, University of Bristol, Bristol BS8 1TS, U.K.;* orcid.org/0000-0001-5080-9535; Email: j.clayden@bristol.ac.uk

Authors

Steven M. Wales − *School of Chemistry, University of Bristol, Bristol BS8 1TS, U.K.;* orcid.org/0000-0003-0637-4225

David T. J. Morris − *School of Chemistry, University of Bristol, Bristol BS8 1TS, U.K.*

Complete contact information is available at: https://pubs.acs.org/10.1021/jacs.1c11928

Notes

The authors declare no competing financial interest.

■ ACKNOWLEDGMENTS

The work was supported by the ERC (AdG DOGMATRON, grant agreement 883786) and the EPSRC (Bristol Centre for Doctoral Training in Chemical Synthesis EP/L015366/1 and Programme Grant "Molecular Robotics" EP/P027067/1).

■ REFERENCES

(1) Berl, V.; Krische, M. J.; Huc, I.; Lehn, J.-M.; Schmutz, M. Template-Induced and Molecular Recognition Directed Hierarchical Generation of Supramolecular Assemblies from Molecular Strands. *Chem.—Eur. J.* **2000**, *6*, 1938−1946.

(2) Morrow, S. M.; Bissette, A. J.; Fletcher, S. P. Transmission of Chirality through Space and across Length Scales. *Nat. Nanotechnol.* **2017**, *12*, 410−419.

(3) Patel, B. H.; Percivalle, C.; Ritson, D. J.; Duffy, C. D.; Sutherland, J. D. Common Origins of RNA, Protein and Lipid Precursors in a Cyanosulfidic Protometabolism. *Nat. Chem.* **2015**, *7*, 301−307.

(4) Magarini, M.; Stano, P. Synthetic Cells Engaged in Molecular Communication: An Opportunity for Modelling Shannon- and Semantic-Information in the Chemical Domain. *Front. Comms. Net.* **2021**, *2*, 48−54.

(5) McCulloch, S. D.; Kunkel, T. A. The Fidelity of DNA Synthesis by Eukaryotic Replicative and Translesion Synthesis Polymerases. *Cell Res.* **2008**, *18*, 148−161.

(6) Palczewski, K. G Protein-Coupled Receptor Rhodopsin. *Annu. Rev. Biochem.* **2006**, *75*, 743−767.

(7) Lovinger, D. M. Communication Networks in the Brain: Neurons, Receptors, Neurotransmitters, and Alcohol. *Alcohol Res. Health* **2008**, *31*, 196−214.

(8) Groves, J. T.; Kuriyan, J. Molecular Mechanisms in Signal Transduction at the Membrane. *Nat. Struct. Mol. Biol.* **2010**, *17*, 659−665.

(9) Ha, J.-H.; Loh, S. N. Protein Conformational Switches: From Nature to Design. *Chem.—Eur. J.* **2012**, *18*, 7984−7999.

(10) Shannon, C. E. A Mathematical Theory of Communication. *Bell Syst. Technol. J.* **1948**, *27*, 623−656.

(11) Barbieri, M. What Is Information? *Philos. Trans. R. Soc.* **2016**, *374*, 20150060.

(12) Fakim, H.; Fabian, M. R. Communication Is Key: 5′−3′ Interactions That Regulate MRNA Translation and Turnover BT. *Adv. Exp. Med. Biol.* **2019**, *1203*, 149−164.

(13) Buddingh', B. C.; Elzinga, J.; van Hest, J. C. M. Intercellular Communication between Artificial Cells by Allosteric Amplification of a Molecular Signal. *Nat. Commun.* **2020**, *11*, 1652.

(14) Yockey, H. P. Origin of Life on Earth and Shannon's Theory of Communication. *Comput. Chem.* **2000**, *24*, 105−123.

(15) Le Bailly, B. A. F.; Clayden, J. Dynamic Foldamer Chemistry. *Chem. Commun.* **2016**, *52*, 4852−4863.

(16) Smulders, M. M. J.; Schenning, A. P. H. J.; Meijer, E. W. Insight into the Mechanisms of Cooperative Self-Assembly: The "Sergeants-and-Soldiers" Principle of Chiral and Achiral C3-Symmetrical Discotic Triamides. *J. Am. Chem. Soc.* **2008**, *130*, 606−611.

(17) Ousaka, N.; Grunder, S.; Castilla, A. M.; Whalley, A. C.; Stoddart, J. F.; Nitschke, J. R. Efficient Long-Range Stereochemical Communication and Cooperative Effects in Self-Assembled Fe4L6 Cages. *J. Am. Chem. Soc.* **2012**, *134*, 15528−15537.

(18) Clayden, J.; Lund, A.; Vallverdu, L.; Helliwell, M. Ultra-Remote Stereocontrol by Conformational Communication of Information along a Carbon Chain. *Nature* **2004**, *431*, 966−971.

(19) Byrne, L.; Solà, J.; Boddaert, T.; Marcelli, T.; Adams, R. W.; Morris, G. A.; Clayden, J. Foldamer-Mediated Remote Stereocontrol: > 1,60 Asymmetric Induction. *Angew. Chem., Int. Ed.* **2014**, *53*, 151−155.

(20) Morris, D. T. J.; Wales, S. M.; Tilly, D. P.; Farrar, E. H. E.; Grayson, M. N.; Ward, J. W.; Clayden, J. A Molecular Communication Channel Consisting of a Single Reversible Chain of Hydrogen Bonds in a Conformationally Flexible Oligomer. *Chem.* **2021**, *7*, 2460−2472.
(21) Nowick, J. S.; Mahrus, S.; Smith, E. M.; Ziller, J. W. Triurea Derivatives of Diethylenetriamine as Potential Templates for the Formation of Artificial *β*-Sheets. *J. Am. Chem. Soc.* **1996**, *118*, 1066−1072.
(22) Lister, F. G. A.; Le Bailly, B. A. F.; Webb, S. J.; Clayden, J. Ligand-Modulated Conformational Switching in a Fully Synthetic Membrane-Bound Receptor. *Nat. Chem.* **2017**, *9*, 420−425.
(23) De Poli, M.; Zawodny, W.; Quinonero, O.; Lorch, M.; Webb, S. J.; Clayden, J. Conformational Photoswitching of a Synthetic Peptide Foldamer Bound within a Phospholipid Bilayer. *Science* **2016**, *352*, 575−580.
(24) Mazzier, D.; Crisma, M.; De Poli, M.; Marafon, G.; Peggion, C.; Clayden, J.; Moretto, A. Helical Foldamers Incorporating Photoswitchable Residues for Light-Mediated Modulation of Conformational Preference. *J. Am. Chem. Soc.* **2016**, *138*, 8007−8018.
(25) Nödling, A. R.; Jakab, G.; Schreiner, P. R.; Hilt, G. ^{31}P NMR Spectroscopically Quantified Hydrogen-Bonding Strength of Thioureas and Their Catalytic Activity in Diels−Alder Reactions. *Eur. J. Org. Chem.* **2014**, *2014*, 6394−6398.
(26) Pike, S. J.; Hutchinson, J. J.; Hunter, C. A. H-Bond Acceptor Parameters for Anions. *J. Am. Chem. Soc.* **2017**, *139*, 6700−6706.
(27) Pike, S. J.; Lavagnini, E.; Varley, L. M.; Cook, J. L.; Hunter, C. A. H-Bond Donor Parameters for Cations. *Chem. Sci.* **2019**, *10*, 5943−5951.
(28) Thordarson, P. Determining Association Constants from Titration Experiments in Supramolecular Chemistry. *Chem. Soc. Rev.* **2011**, *40*, 1305−1323.
(29) Hunter, C. A. Quantifying Intermolecular Interactions: Guidelines for the Molecular Recognition Toolbox. *Angew. Chem., Int. Ed.* **2004**, *43*, 5310−5324. The slightly reduced $\Delta\delta_P$ of Bu_3PO with the mixture of **3** and **5** is presumably due to weakly competitive intermolecular binding of **3** to the available carbonyl group of the trisubstituted urea in **5** (representative β = 8.3 for a urea carbonyl groups: see ref 29). Adding **5** (1 equiv) to **3** (10 mM, CD_2Cl_2) led to downfield shifts of both the alkyl- and aryl-N−H signals of **3** in the ^{1}H NMR spectrum ($\Delta\delta_H$ = +0.44 and +0.76 ppm, respectively; Figure S24), providing qualitative evidence of a binding interaction.
(30) The chemical shift of this ion pair matched closely that of an authentic sample of the tetraarylborate $[t\text{-BuHN-P}(NMe_2)_3]^+\cdot[BAr^F{}_4]^-$ prepared separately (δ_P = 34.71 ppm, Figure S29).
(31) To validate this interpretation, we confirmed that the presence of $[t\text{-BuHN−P}(NMe_2)_3]^+\cdot\mathbf{4}^-$ in the absence of **3** does not affect the chemical shift of Bu_3PO ($\Delta\delta_P$ = −0.07 ppm, Figure S35).
(32) Wegner, A. Head to Tail Polymerization of Actin. *J. Mol. Biol.* **1976**, *108*, 139−150.
(33) Diemoz, K. M.; Franz, A. K. NMR Quantification of Hydrogen-Bond-Activating Effects for Organocatalysts Including Boronic Acids. *J. Org. Chem.* **2019**, *84*, 1126−1138.
(34) Walvoord, R. R.; Huynh, P. N. H.; Kozlowski, M. C. Quantification of Electrophilic Activation by Hydrogen-Bonding Organocatalysts. *J. Am. Chem. Soc.* **2014**, *136*, 16055−16065.

https://doi.org/10.1021/jacs.1c11928
J. Am. Chem. Soc. 2022, 144, 2841−2846